Lab on a Chip

Miniaturisation for chemistry, physics, biology, materials science and bioengineering

www.rsc.org/loc

Volume 11 | Number 23 | 7 December 2011 | Pages 3923–4128

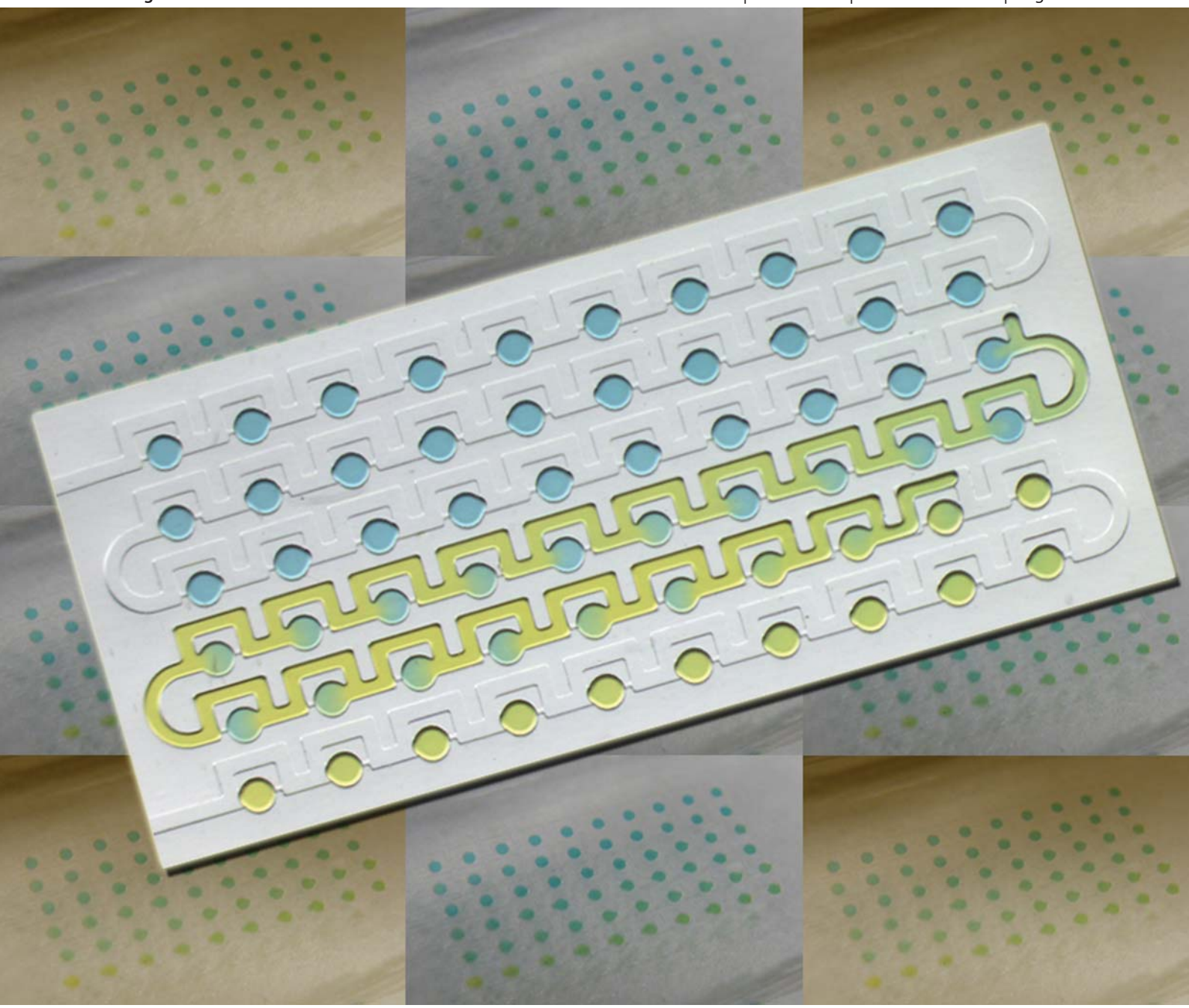

ISSN 1473-0197

RSC Publishing

COMMUNICATION

Vanapalli *et al.*

Microfluidic static droplet arrays with tuneable gradients in material composition

1473-0197(2011)11:23;1-0

Lab on a Chip

Dynamic Article Links

Cite this: *Lab Chip*, 2011, **11**, 3949

www.rsc.org/loc

COMMUNICATION

Microfluidic static droplet arrays with tuneable gradients in material composition†

Meng Sun, Swastika S. Bithi and Siva A. Vanapalli*

Received 1st August 2011, Accepted 28th September 2011
DOI: 10.1039/c1lc20709a

We describe a one-step passive strategy to create concentration gradients in static droplet arrays. The technique exploits controlled exchange of materials between moving plugs and stationary drops. The concentration of soluble reagents can be varied from drop-to-drop in the presence of other soluble reagents or insoluble materials (*e.g.* cells) at well-defined time points.

Demand for high-throughput screening (HTS) is pervasive in applications related to chemistry, biology, medicine and biomaterials.[1–5] Droplet-based microfluidics[6–10] is emerging as a powerful and inexpensive alternative to conventional multi-well-plate-based screening, offering significant opportunities to compartmentalize reactions in very small volumes with flexible control of composition. Current methods to manipulate reagent concentration in drops fall under two broad categories - mobile droplet arrays (MDAs) and static droplet arrays (SDAs).[10] In mobile droplet arrays (MDAs), drops are continuously produced using microfluidic methods and flow past a detector. The drop composition is tuned by either adding reagents prior to drop production[11–17] or by coalescing reagent-loaded drops downstream using external fields (*e.g.* fluid pressure or electric fields).[18–20] However, some of the MDA methods suffer from either narrow concentration range (typically two orders of magnitude or less),[12–14] or lack the ability to directly produce concentration gradients in drops containing larger insoluble materials such as living cells,[15–18] limiting their applicability to cell-based assays. More importantly, MDA methods have difficulties with indexing drop position or acquiring time-lapse data for assays of long duration.

Unlike MDAs, two-dimensional SDAs mimic multi-well plates with the distinction that nanolitre to picolitre-scale drops are stored at predefined locations.[21–29] This method allows simultaneous monitoring of many individual reactions in drops over a wide range of timescales. Sample evaporation is also reduced significantly in an enclosed substrate. Moreover, the drop position is indexed if further manipulation is needed. However, current SDAs are largely limited to generating arrays of drops containing a target sample (*e.g.* enzymes, DNA, bacteria, small animals) in the presence of only single concentration of a soluble reagent,[21–26] precluding their application to HTS. By coupling permeation-driven transport across membranes,[30,31] additional flexibility has been achieved in tuning drop content, however, these systems require complex multilayer devices and are limited to reagents that permeate through the membrane. Thus, there is a tremendous need for low-cost and simple approaches to (i) vary the concentration of reagents in a tunable manner from drop-to-drop in an array, and (ii) add or remove soluble reagents from a SDA at well defined time-points to execute multi-step assays. If these capabilities are realized, the power of SDAs can be expanded to HTS and other lab-on-chip technologies. Here we describe a method that delivers these capabilities.

The basic idea of our method involves exchange of materials between stationary drops and moving plugs. In Fig. 1 we illustrate our method with a representative dilution experiment. To perform dilution, we built a reagent-loaded cartridge[32] (Fig. 1a, left) containing 'sample' (dye in our experiments) plug and water as diluting plug, separated by an oil phase. The plugs from the cartridge are delivered into the microfluidic device that is prefilled with oil (see Fig. 1a, center). The device contains a microchannel network with a repeated sequence of loops (Fig. 1b). Each loop contains a bypass channel having lower hydrodynamic resistance than the branch containing the fluidic trap[23,24,33] (see inset, Fig. 1b). Details of the geometry dimensions are provided in Supplementary Information (Section 1).

The principle of generating a droplet array with a sample plug in this network has been described previously.[24] Briefly, the sample plug moves into the bypass channel, enhancing the hydrodynamic resistance of the bypass, which allows a portion of the sample plug to fill the fluidic trap. Further movement of the plug in the trap is restricted by the capillary pressure at the geometric constriction. As the plug continues to traverse other loops, eventually the tail of the plug reaches the junction of each loop, undergoes break-up and generates immobilized droplets of uniform composition. Fig. 1b shows the time-sequence of this process (also see Supplementary Movie S1).

The key novelty of this work lies in combining the above process of generating droplet arrays with the capability of adding reagents by using a cartridge. Concentration gradients in the array are produced *via* a unique mechanism of coalescence, mixing and break-up of additional plugs with the preformed array of homogeneous composition (see Supplementary Movie S2). Basic description of the dilution process is as follows. When the water plug arrives into the network, it proceeds into the bypass channel as shown in Fig. 1c. However, after the head of the plug advances into the bypass channel, the thin film of oil between the stationary drop and the

Department of Chemical Engineering, Texas Tech University, Lubbock, TX, 79409-3121, USA. E-mail: siva.vanapalli@ttu.edu; Fax: +1-806-742-3552; Tel: +1-806-742-1757

† Electronic supplementary information (ESI) available: Experimental section; effect of surfactant concentration on rupture time; three movies illustrating the trapping and diluting processes and reagent exchange dynamics. See DOI: 10.1039/c1lc20709a

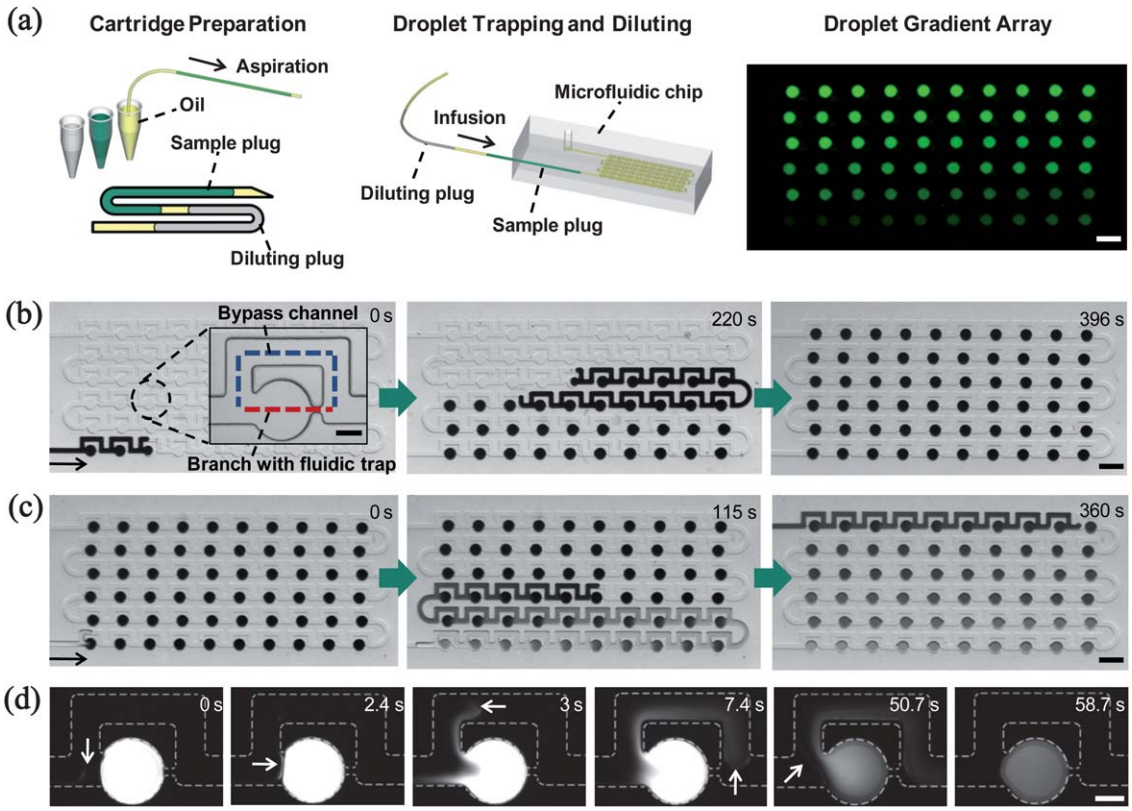

Fig. 1 Principle of generation of static droplet arrays with tuneable composition. (a) Schematic illustration of (left) cartridge preparation by aspiration and (center) introduction of plugs into the microfluidic device for droplet trapping with subsequent dilution, (right) a droplet gradient array generated by trapping fluorescent droplets (10^{-4} M sodium-derivative of fluorescein) followed by dilution with a 2.2-μL-water plug at flow rate of 0.5 μL min^{-1}. (b) Images illustrating the motion of the sample (black food dye) in the fluidic network. The inset of (b) shows the loop design with the bypass channel (blue line) and the fluidic trap (red line). (c) Time-sequence snapshots of the dynamics of gradient generation by the diluting plug in the fluidic network. The time stamps are shown in the top right corner of each image. (d) Time-sequence snapshots of the dynamics of diluting water plug coalescence with the sample droplet. The arrows in the images identify the location of the front and end of the diluting plug. The trapped droplet contains a fluorescent dye (10^{-3} M sodium-derivative of fluorescein) and dilution was performed by a 0.8-μL-water plug at flow rate of 0.5 μL min^{-1}. Continuous phase is 0.1% (w/v) Span 80 in mineral oil. Scale bars in (a–c) are 1 mm; scale bars in inset of (b) and (d) is 200 μm.

moving plug ruptures allowing exchange of materials between the drop and the plug. This exchange dynamics is shown in Fig. 1d (also see Supplementary Movie S3). Material is exchanged at every loop-junction as the water plug travels through the network causing a gradient of soluble material in the water plug (Fig. 1c). Because the first drop gets diluted with water and the successive drops get diluted with increasing amounts of soluble material, we observe concentration gradient in the array. The method offers the flexibility of either increasing or decreasing the concentration of the soluble material from drop-to-drop in the array, by simply changing the initial composition of the moving plug. Fig. 1a (right) shows a representative droplet gradient array resulting from this process.

The factors affecting the fluidic-trapping and gradient-generation processes include the network geometry, fluid properties (viscosity ratio and surfactant concentration) and carrier fluid flow rate. Specifically: (i) At a given carrier fluid flow rate, the flow resistance ratio of the branches in the loop coupled with the hydrodynamic resistance of the plug affect the formation of immobilized arrays. The carrier fluid flow rate needs to be optimized to retain the drops in the traps, as discussed in our earlier work[33] (ii) Surfactant concentration controls the coalescence ability (see Supplementary Information, Section 5). It also modifies the hydrodynamic resistance of the moving plug, affecting the trapping process[34] (iii) For a given network geometry, the fluid properties coupled with the flow conditions determine the final gradient in the SDA as these factors influence the time allowed for continuous advection of the material from stationary drops and the extent of recirculation-induced mixing in the moving plug. For the network geometry investigated in this work, a flow resistance ratio of ≈ 1.5–3, surfactant (Span 80) concentration of 0–0.5% and carrier fluid flow rate of 0.2–2 μL min^{-1} was found to be optimal for the dilution mechanism to operate.

Several control parameters are available to tune the concentration gradient and range in the array, lending flexibility to the approach. Importantly, small variations in concentration from drop-to-drop can be accessed either across a narrow or large range. In particular, lower flow rates yield a wider range and steeper gradient because of the increased duration for dilution (Fig. 2a). In addition, plug volume (Fig. 2b) or the number of diluting plugs (Fig. 2c) can be varied to manipulate reagent concentration in drops. We find the gradients to be reproducible as three independent measurements at the condition of 1.0 μL min^{-1} in Fig. 1a, yielded a standard deviation of less than 4%. Because of the ability to deliver multiple plugs at well-defined time points, spatial concentration gradients can be generated in a time varying manner. This unique aspect could be particularly useful to interrogate the response of living systems to temporal variations in soluble signals.[31,35]

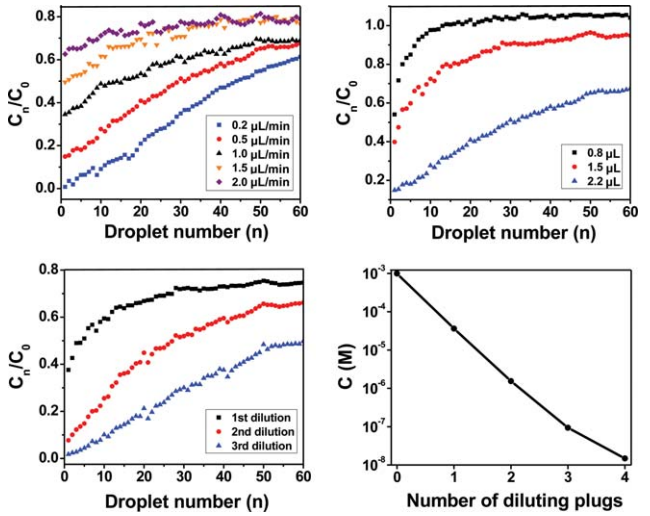

Fig. 2 Control of concentration gradients by varying system parameters. In (a–c), we define C_0 as the initial concentration of black dye in the trapped drops before the dilution and C_n as the concentration of dye in each drop after the dilution (n = 1–60). The dye concentration was estimated from the grey-scale intensity values. To generate this data a solution of black dye was used as the sample plug and water was used as the diluting plug. (a) The diluting plug volume (2.2-μL) was fixed and flow rate was varied. (b) The flow rate was fixed (0.5 μL min^{-1}) and the diluting plug volume varied. (c) The flow rate (0.5 μL min^{-1}) and diluting volume (1.5-μL) were fixed but the number of dilutions varied. (d) Variation in concentration of fluorescent dye in the first droplet in an array as a function of number of dilutions. The starting concentration of the drop was 10^{-3} M of fluorescein (sodium derivative) and dilutions were performed sequentially by using four 2.2-μL-water plugs at a flow rate of 0.5 μL min^{-1}. Continuous phase is 0.1% (w/v) Span 80 in mineral oil.

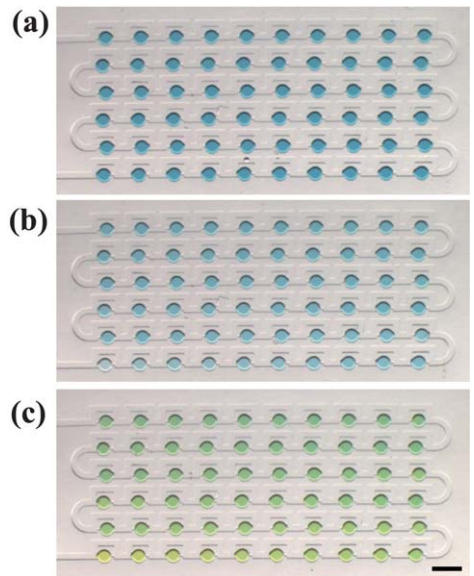

Fig. 3 Static droplet arrays of multi-component mixtures. (a) SDA containing blue dye. (b) The SDA in (a) is diluted with a 2.2-μL water plug to generate a concentration gradient of blue dye. (c) The SDA in (b) is diluted with a 2.2-μL yellow dye plug to generate concentration gradients in both blue and yellow dyes. Flow rates in (a), (b) and (c) are 1 μL min^{-1}, 1 μL min^{-1}, and 0.5 μL min^{-1} respectively. Continuous phase is 0.1% (w/v) Span 80 in mineral oil. Scale bar: 1 mm.

Our method is capable of delivering a wide concentration range that is only limited by the detection method. This remarkable ability is because of continuous sample removal from the first drop and not so much from the last drop in the array. To quantify a practical bound on dilution, we generated an array containing a uniform composition of a fluorescent dye, diluted it with 4 water plugs of the same volume and monitored the reduction in fluorescence of the first droplet in the array (See Supplementary Information Section 6). As shown in Fig. 2d, we detect nearly 100,000-fold dilution of the first droplet. This orders of magnitude concentration variation illustrates the power of the method for screening applications.

Because of the ability to add or remove materials from a drop, our technique is also conducive to producing multi-component arrays, which is a key aspect of HTS applications. To demonstrate this feature, we constructed a 3-plug cartridge containing a water plug flanked by two reagent plugs (blue and yellow dyes). In Fig. 3a we show an SDA with a uniform composition of blue dye, which was subsequently diluted with water (Fig. 3b). Adding a yellow reagent plug produces a decreasing concentration of yellow and an increasing concentration of blue in the array, yielding gradients in both the reagents (Fig. 3c). In fact, the approach can be extended to any number of reagent gradients by introducing additional plugs in the cartridge. This ease of generating arrays with multi-component gradients comes at the cost of reduced independent control over the composition of each reagent.

Numerous high throughput applications handle more complex materials than soluble reagents. For example, in drug screening, a population of cells is exposed to a wide range of drug concentrations to identify the optimal dosage. In Fig. 4, we illustrate that our method is capable of creating gradients of a soluble reagent in drops containing insoluble materials (see Fig. 4). In one experiment, we injected first the soluble reagent plug, followed by 0.2 μm and 1 μm colloidal plugs. The results indicate a gradient of soluble material (red dye) in a drop containing a uniform dispersion of 1 μm and 0.2 μm particles (Fig. 4a). We also tested this approach with cell suspensions by encapsulating a mixture of leukemia cells and trypan blue dye in individual drops and capturing them in an array. Subsequently, the array was diluted with a phosphate buffer saline plug to produce a gradient of trypan blue (Fig. 4b). Despite the initial concentration of cells being low (average of 8 cells/drop) compared to particle experiments, the dilution step did not remove cells from all the drops. We find 90% of the drops to contain one or more cells. This unexpected finding implies different rates of transport for soluble and larger insoluble materials, motivating future investigation of the complex hydrodynamics involved.

An important aspect dictating the suitability of our method to specific applications is the time-scale of gradient development, since reactions may initiate when the sample and dilute plugs contact each other. We find in our device, concentration gradients for each drop are established in 1–5 mins (see Fig. 1c,d). Although this time-scale is inappropriate for assays involving very fast kinetics, the mixing time-scales in our method suffice for a broad range of applications including cytotoxicity assays, protein crystallization and DNA binding assays. For such assays, the format of our device allows detection based on both camera-based as well as photodiode-based systems, in which the signals could come from readouts such as fluorescence or luminescence.

In summary, we developed a new method that is capable of modulating reagent concentration by 5 orders of magnitude in SDA and also producing multi-component mixtures. Implementation of the technique is straightforward and requires minimal resources - the

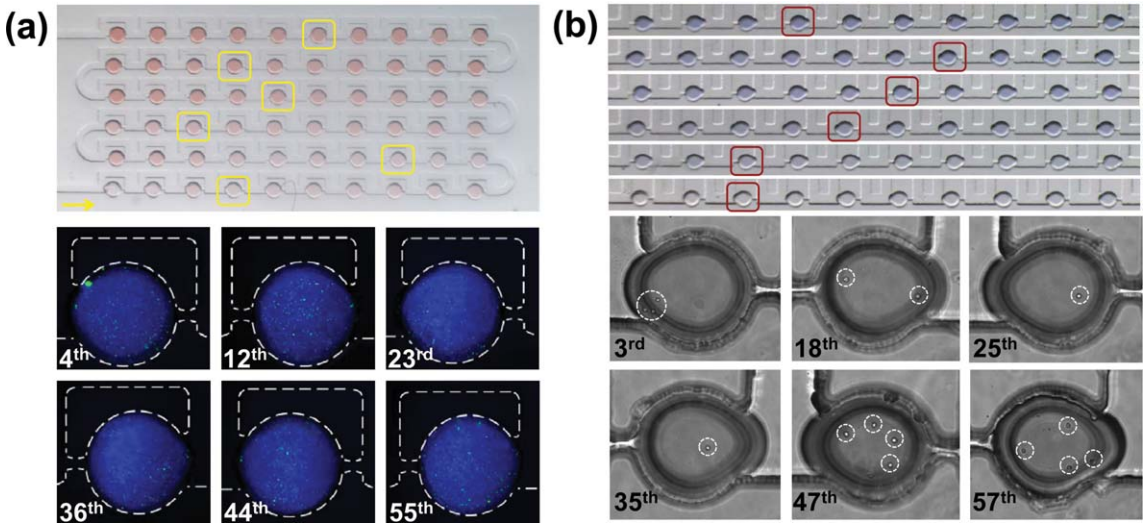

Fig. 4 Static droplet gradient arrays with colloidal particles and cells. (a) The experiment consisted of creating a SDA with uniform composition of red dye, with subsequent dilution with 0.2 μm (blue fluorescent) and 1 μm (green fluorescent) colloids sequentially at the flow rate of 1 μL min^{-1}. The top frame shows the bright field image of the final composition of the array showing the visible gradient in red dye (colloids are not visible). The bottom frames show fluorescent images of selected drops in the array highlighting the presence of both the blue and green colored colloids. (b) The top frame shows the SDA containing leukemia cells with a gradient in dye (trypan blue). The bottom frames show the selected droplets containing cells (marked by circles). In (a) and (b) the selected droplets are highlighted by boxes. Continuous phase is 0.1% (w/v) Span 80 in mineral oil. Scale bars in upper and lower images in (a) and (b) are 1 mm and 100 μm.

microfluidic device, a reagent-cartridge and a pump. In this work, we demonstrated a throughput of nearly 60 different concentrations (in 30 nL drops) in about 10 min using only 2 μL of sample volume. We believe our approach is scalable beyond 60 drops to 10^3 drops by increasing the device footprint and multiplexing. These next generation devices could serve as an inexpensive alternative to robot-aided fluid dilution benefitting a wide range of HTS applications.

Acknowledgements

We acknowledge National Science Foundation (CBET: 0967172 and 0932796) and Cancer Prevention and Research Institute of Texas (CPRIT: RP100756) for partially supporting this work. We thank Raul Martinez-Zaguilan for providing the leukemia cells. We are grateful to Jerzy Blawzdziewicz, Ziena Khan and William Wang for critical reading of the manuscript.

Notes and references

1 J. Inglese, R. L. Johnson, A. Simeonov, M. Xia, W. Zheng, C. P. Austin and D. S. Auld, *Nat. Chem. Biol.*, 2007, **3**, 466.
2 J. Hong, J. B. Edel and A. J. deMello, *Drug Discovery Today*, 2009, **14**, 134.
3 D. G. Anderson, S. Levenberg and R. Langer, *Nat. Biotechnol.*, 2004, **22**, 863.
4 R. Macarron, M. N. Banks, D. Bojanic, D. J. Burns, D. A. Cirovic, T. Garyantes, D. V. S. Green, R. P. Hertzberg, W. P. Janzen, J. W. Paslay, U. Schopfer and G. S. Sittampalam, *Nat. Rev. Drug Discovery*, 2011, **10**, 188.
5 C. G. Simon and S. Lin-Gibson, *Adv. Mater.*, 2011, **23**, 369.
6 H. Song, D. L. Chen and R. F. Ismagilov, *Angew. Chem., Int. Ed.*, 2006, **45**, 7336.
7 S. Y. Teh, R. Lin, L. H. Hung and A. P. Lee, *Lab Chip*, 2008, **8**, 198.
8 D. T. Chiu, R. M. Lorenz and G. D. M. Jeffries, *Anal. Chem.*, 2009, **81**, 5111.
9 J. J. Agresti, E. Antipov, A. R. Abate, K. Ahn, A. C. Rowat, J. C. Baret, M. Marquez, A. M. Klibanov, A. D. Griffiths and D. A. Weitz, *Proc. Natl. Acad. Sci. U. S. A.*, 2010, **107**, 4004.
10 R. R. Pompano, W. S. Liu, W. B. Du and R. F. Ismagilov, *Annu. Rev. Anal. Chem.*, 2011, **4**, 59.
11 M. Sun and Q. Fang, *Lab Chip*, 2010, **10**, 2864.
12 H. Song and R. F. Ismagilov, *J. Am. Chem. Soc.*, 2003, **125**, 14613.
13 R. M. Lorenz, G. S. Fiorini, G. D. M. Jeffries, D. S. W. Lim, M. Y. He and D. T. Chiu, *Anal. Chim. Acta*, 2008, **630**, 124.
14 N. Damean, L. F. Olguin, F. Hollfelder, C. Abell and W. T. S. Huck, *Lab Chip*, 2009, **9**, 1707.
15 L. F. Cai and Q. Fang, *MicroTAS 2010*, Groningen, The Netherlands, 2010, pp. 1814.
16 J. S. Edgar, G. Milne, Y. Q. Zhao, C. P. Pabbati, D. S. W. Lim and D. T. Chiu, *Angew. Chem., Int. Ed.*, 2009, **48**, 2719.
17 A. B. Theberge, G. Whyte and W. T. S. Huck, *Anal. Chem.*, 2010, **82**, 3449.
18 X. Z. Niu, F. Gielen, J. B. Edel and A. J. deMello, *Nat. Chem.*, 2011, **3**, 437.
19 I. Shestopalov, J. D. Tice and R. F. Ismagilov, *Lab Chip*, 2004, **4**, 316.
20 A. R. Abate, T. Hung, P. Mary, J. J. Agresti and D. A. Weitz, *Proc. Natl. Acad. Sci. U. S. A.*, 2010, **107**, 19163.
21 A. Huebner, D. Bratton, G. Whyte, M. Yang, A. J. deMello, C. Abell and F. Hollfelder, *Lab Chip*, 2009, **9**, 692.
22 C. H. J. Schmitz, A. C. Rowat, S. Koster and D. A. Weitz, *Lab Chip*, 2009, **9**, 44.
23 W. W. Shi, J. H. Qin, N. N. Ye and B. C. Lin, *Lab Chip*, 2008, **8**, 1432.
24 H. Boukellal, S. Selimovic, Y. W. Jia, G. Cristobal and S. Fraden, *Lab Chip*, 2009, **9**, 331.
25 P. Abbyad, R. Dangla, A. Alexandrou and C. N. Baroud, *Lab Chip*, 2011, **11**, 813.
26 D. E. Cohen, T. Schneider, M. Wang and D. T. Chiu, *Anal. Chem.*, 2010, **82**, 5707.
27 J. U. Shim, G. Cristobal, D. R. Link, T. Thorsen and S. Fraden, *Cryst. Growth Des.*, 2007, **7**, 2192.
28 W. B. Du, M. Sun, S. Q. Gu, Y. Zhu and Q. Fang, *Anal. Chem.*, 2010, **82**, 9941.
29 W. B. Du, L. Li, K. P. Nichols and R. F. Ismagilov, *Lab Chip*, 2009, **9**, 2286.
30 S. Selimovic, F. Gobeaux and S. Fraden, *Lab Chip*, 2010, **10**, 1696.
31 J. U. Shim, S. N. Patil, J. T. Hodgkinson, S. D. Bowden, D. R. Spring, M. Welch, W. T. S. Huck, F. Hollfelder and C. Abell, *Lab Chip*, 2011, **11**, 1132.
32 L. Li, D. Mustafi, Q. Fu, V. Tereshko, D. L. L. Chen, J. D. Tice and R. F. Ismagilov, *Proc. Natl. Acad. Sci. U. S. A.*, 2006, **103**, 19243.
33 S. S. Bithi and S. A. Vanapalli, *Biomicrofluidics*, 2010, **4**, 044110.
34 M. J. Fuerstman, A. Lai, M. E. Thurlow, S. S. Shevkoplyas, H. A. Stone and G. M. Whitesides, *Lab Chip*, 2007, **7**, 1479.
35 J. El-Ali, P. K. Sorger and K. F. Jensen, *Nature*, 2006, **442**, 403.

